
Book Section:
Marvin, Andy orcid.org/0000-0003-2590-5335, Armstrong, Robert and Dawson, John Frederick orcid.org/0000-0003-4537-9977 (2011) An Experimental Investigation of the use of Q-Factor to Determine the Shielding Effectiveness of Electrically Large Equipment Enclosures with Apertures. In: EMC Europe 2011 York, Proceedings of. , GBR , p. 148.

Proc. of the 10th Int. Symposium on Electromagnetic Compatibility (EMC Europe 2011), York, UK, September 26 – 30, 2011

An Experimental Investigation of the use of Q-Factor to Determine the Shielding Effectiveness of Electrically Large Equipment Enclosures with Apertures

Rob Armstrong, Andy Marvin and John Dawson
Department of Electronics
University of York
York, United Kingdom

***Abstract*—The current method of obtaining a Shielding Effectiveness (SE) measurement involves field measurements both inside and outside the enclosure to be tested. In this paper, a relationship between the Shielding Effectiveness and the Q-factor of the enclosure under test (EUT) is investigated. Measurements are made in an anechoic chamber to obtain the Q-factor using a method previously detailed and to assess the Shielding Effectiveness of the enclosure under test. A relationship between Q-factor and shielding effectiveness is shown, and possible uses of this relationship are discussed.**

Keywords — Q-factor, Anechoic chamber, Shielding Effectiveness measurement.

I. INTRODUCTION

Shielding Effectiveness (SE) measurements of equipment enclosures are a necessary part of informing equipment design. The current method used for obtaining a value for the SE is to measure the received power inside the Enclosure under Test (EUT) and compare it to the received power from outside the EUT. This is usually expressed in dB using the following relationship [1]:

$$SE = 10\log_{10}\left(\frac{P_{out}}{P_{in}}\right) \qquad (1)$$

where P_{out} and P_{in} are the powers received by probe antennas outside and inside the EUT respectively. Appropriate antenna corrections are used. Typically measurements may be made in reverberation chambers with the EUT acting as a nested reverberation chamber stirred by its own internal stirrer. The SE is dependent on the configuration of the apertures in the EUT; as the aperture size increases, so does the received internal power, thus lowering the SE.

For this method and equation to be valid, the EUT has to be classed as an electrically large reverberation chamber. Reverberation chambers have metallic, highly electrically reflective walls, which, in conjunction with a mode stirring method, to produce statistically uniform internal electromagnetic fields. Either mechanical or electronic mode stirring can be used to obtain statistical field uniformity; in this case the method is mechanical stirring, with a stirrer situated inside the EUT.

For the stirring to be effective and to provide an adequately uniform field, the chamber must be of sufficient size to enable the creation of around 60 resonant modes [1,2]. This leads to there being a minimum frequency to obtain enough resonant modes to get statistically uniform fields. For the EUT used here (dimensions of 0.48m x 0.48m x 0.12m) the minimum frequency for 60 resonant modes is 1.9GHz. The experiments here are carried out at 4GHz to make absolutely sure there are enough resonant modes present for the EUT to be in an overmoded state.

Hill et al [3] describe the average Q-factor of an electrically large reverberation chamber. The reciprocal of the average Q-factor is shown to be the sum of the contributions, shown in (2). The inverse nature of this relationship means that the smallest of the values of Q-factor becomes the dominant contributor.

$$Q^{-1} = Q_1^{-1} + Q_2^{-1} + Q_3^{-1} + Q_4^{-1} \qquad (2)$$

Here, the average value of Q-factor is made up from the following effects: Q_1 represents the losses in the cavity walls, Q_2 is the absorption loss stemming from any absorbing material contents inside the chamber, Q_3 concerns the losses associated with any apertures, and finally Q_4 encompasses the losses in the measurement antennas.

The value for Q_1 is obtained from averaging plane wave losses in the enclosure walls over all angles of incidence and all polarizations [3], giving the result of

$$Q_1 = \frac{3V}{2\mu_r S\delta} \qquad (3)$$

The Department of Electronics at the University of York and York EMC Services Ltd. support this work through a PhD stipend.

where μ_r is the relative permeability of the wall material (in this case, brass), S is the surface area and V the volume of the EUT and δ is the skin depth. We estimate Q_1 is of the order of 10^5 for our EUT. The Q_1 contribution to the total Q-factor is purely dependent on the size and material of the enclosure, which has minimal change throughout this experiment. The surface area S will change if the apertures are very large, which can contribute to a different Q-factor for different aperture configurations. This change in S is small compared to the contribution of Q_3, however.

These experiments are done with nothing inside the EUT other than the mechanical stirrer paddle (the control motor is situated on the outside the EUT) and so there is little if no absorption loss inside the EUT i.e. Q_2 is very large, therefore Q_2^{-1} is vanishingly small.

The interesting contribution for the purposes of comparing Q-factor to SE is the aperture contribution Q_3, given in Equation 4

$$Q_3 = \frac{4\pi V}{\lambda < \sigma_1 >} \qquad (4)$$

where V is the volume of the chamber, λ is the wavelength and $<\sigma_1>$ is the averaged transmission cross section of the aperture in question. For electrically large apertures, $<\sigma_1>$ is independent of frequency; meaning Q_3 is proportional to frequency.

If the aperture under examination is of arbitrary shape and is assumed to be in a flat infinitely large conducting panel of zero thickness then aperture theory [4] provides a way of obtaining $<\sigma_1>$. Using the geometric optics approximation and restricting the integral over the incident elevation angles to $\pi/2$ (as the aperture is only exposed to the field on one side), a value for $<\sigma_1>$ can be obtained. This relationship turns out simply as Equation 5 with A as the area of the aperture. This is only valid provided the aperture is electrically large and non resonant.

$$< \sigma_1 >= \frac{A}{2} \qquad (5)$$

The treatment for electrically small apertures is similarly derivable, however the cross section for a resonant aperture is not a simple relationship. With the exception of the "small hole" configuration, see Figure 1, all apertures in these experiments are electrically large at 4GHz.

The value of Q_4 is dependent on the antenna impedance mismatch m, as shown in Equation 6.

$$Q_4 = \frac{16\pi^2 V}{m\lambda^3} \qquad (6)$$

At higher frequencies, Q_4 becomes larger due to the wavelength dependence. For this EUT and the antennas used we estimate that Q_4 is of the order of 10^4. This value is a result of the antenna mismatch factor m, calculated from the reflection coefficient from the *S11* parameter. This means that Q_1 and Q_4 have to be taken into account unless the aperture losses are large and Q_3 is small enough to dominate Equation (2).

The only value in Equation 2 that changes throughout these experiments is that of the aperture losses Q_3; the others apart from Q_1 can be assumed to stay constant over such a small measurement bandwidth. As mentioned, the surface area term in Q_1 may become significant at larger aperture sizes.

In this paper we examine the relationship between the dominant Q_3 and the measured SE and propose a measurement of SE based on the observed Q-factor.

II. Obtaining The SE Measurement

Data is taken in an anechoic chamber of dimensions 1.8 x 1.8m x 3m with the EUT 2m away from the external antenna The EUT in the chamber is shown in Figure 2. A Network Analyser measures the S21 and S11 parameters at 4GHz. These parameters refer to the coupling between the monopole antenna inside the stirred EUT and the external ridged waveguide horn antenna in the anechoic chamber. A single 19mm monopole antenna measures the received power inside the EUT.

The level of field coupling into the EUT from the horn antenna is and hence the SE is controlled by changing the layout and configuration of apertures on the front panel of the EUT. The different aperture layouts are shown in Figure 1. Data is taken from the EUT using the Network Analyser (NA) around 4GHz using two different scan bandwidths, 50MHz and 100MHz each with the maximum 1601 data points. This is done to investigate the effect of the number of resonant modes seen by the NA on the average Q-factor; the 50MHz span will encompass less resonant modes than the 100MHz span.

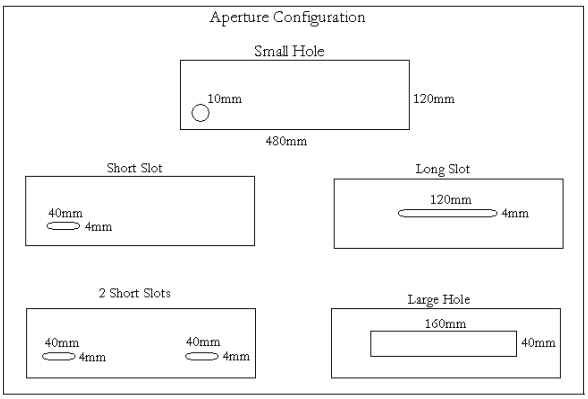

Figure 1: Aperture Configuration used on the front panel of the EUT to provide differing levels of shielding. Also used was a "No holes" configuration with all apertures sealed. These configurations provide the 6 points in Figure 5.

To obtain an SE measurement, the electric field power inside the EUT P_{in} is compared to the electric field power outside the EUT P_{out}, as per Equation (1). The EUT is mechanically mode stirred using a stepper motor and a small paddle stirrer to ensure that the P_{in} measurement is not dependent on position inside the EUT. Data is taken while the stepper motor is stopped to ensure that there is no interference from noise on the motor. The paddle is inside the working volume of the EUT with the motor on the outside; the control hardware sits outside the chamber and is connected via a shielded control cable. The stirrer has 400 steps per revolution; statistically independent data sets are taken every 2 steps, giving 200 measurement sets per full rotation of the stirrer paddles. The data sets are averaged over one full stirrer rotation to obtain the average field power inside the EUT. As the EUT is being effectively stirred, this makes the positioning of the receiving monopole antenna irrelevant within the working volume of the EUT.

The P_{out} measurement is also taken using a 19mm monopole receiving antenna on an electrically large ground plane. The EUT is replaced with the ground plane for this measurement, with the P_{out} receiving monopole positioned where the working volume of the EUT would be, were the EUT present during the measurement. The SE is then calculated using Equation (1). The Anechoic chamber turntable mechanism is not used during either measurement. In this preliminary study, the main interest of this paper in is how the different aperture configurations change the SE, not the absolute value of the SE. The different aperture configurations are only on the front panel facing the external ridged waveguide horn antenna, and the EUT is mode stirred internally. The measured SE in an anechoic chamber with this set-up will depend on the directional properties of the array of apertures considered as an antenna. As only one EUT orientation is used our results are comparative and indicate changes in SE as the aperture configuration is changed. The S11 correction is used on the SE measurement as detailed in [5] for both antenna configurations.

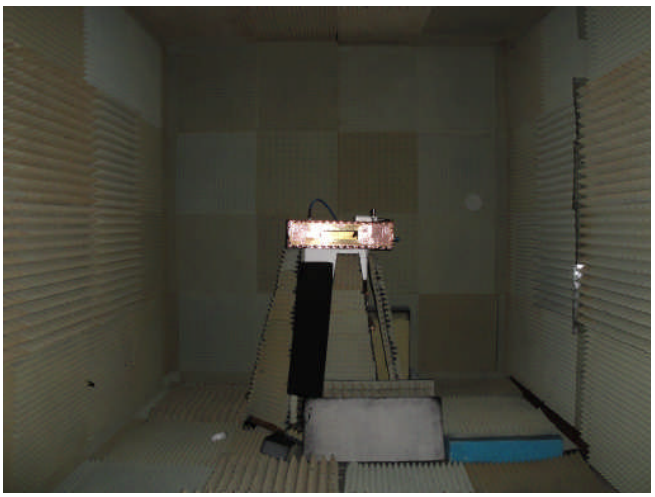

Figure 2: EUT in place in the anechoic chamber. The front panel is facing the camera and the ridged waveguide antenna – current aperture configuration is "Large Hole".

III. Obtaining the Q-Factor

The Q-factor is calculated using the frequency response of each data set from the stirred EUT. The autocorrelation of the frequency response at each stirrer position is taken from the recorded data using a MatLab program. The Width of Autocorrelation (WA) [6] is found for various 'cut-off levels', 1.2dB, 2dB, 2.5dB and 3dB at each stirrer position. This leads to 200 values for WA, which are then averaged over the full stirrer rotation. This results in an average WA for each cut-off level, and is carried out independently for both the 50MHz and 100MHz spans.

It has been shown [7] that as the average Q-factor decreases, the width of the autocorrelation peak increases. An example autocorrelation peak is shown in Figure 3, a plot of the autocorrelation of the frequency response of the EUT at 4GHz and with the 'large hole' configuration. The four different cut-off levels can be seen in Figure 3.

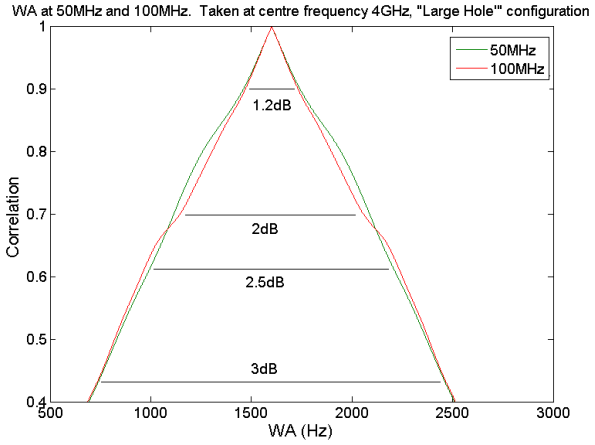

Figure 3: Autocorrelation plot for the "large hole" configuration at 4GHz, showing the two autocorrelation traces at 50MHz and 100MHz measurement bandwidth. The ordinate is normalised to 1.

It can be seen in Figure 3 that a 'shouldering' effect of the 100MHz autocorrelation plot is occurring between the 2dB and 2.5dB cut-off levels. This shouldering effect moves around – note that the 50MHz shoulder is higher up on the autocorrelation plot – and highlights the need to look at the different cut-off levels. The shouldering effect is more apparent at higher frequencies. The merits of the different cut-off levels are as follows. The 1.2dB cut-off level has the advantage of being clear of any shouldering effects, which tend to occur below this cut-off level. The disadvantage of the 1.2dB level being used as a measure of WA is that the sensitivity is not as good. By this it is meant that the WA will not change very much for a given change in autocorrelation plot width. By contrast, it would seem that the 3dB cut-off level would be the best for obtaining the

largest change in WA. However, it can be seen from Figure 3 that the traces for both 50MHz and 100MHz are similar at the 3dB level. This level is also very susceptible to the shouldering effects. The 2dB and the 2.5dB levels could be seen as a compromise between the low sensitivity of the 1.2dB and the poor resistance to the shouldering effect of the 3dB level. However, it can be seen in Figure 3 that there are fairly major shouldering effects present at both the 2dB and the 2.5dB levels. This would tend to indicate that the best cut-off level to be used is the 1.2dB level, for accurate results albeit with reduced sensitivity.

The first step to obtaining a value for the Q-factor from the WA is to simulate a WA for a given Q-factor. A simulation program used in [7] computes the theoretical frequency response for any cavity for a given value of Q-factor. This theoretical frequency response is calculated by combining all of the many resonant modes present in the EUT. The modes are assumed to have Lorenzian line shape. The WA can then be calculated from the autocorrelation of this theoretical frequency response, giving a table of Q-factor vs. WA for each data set. This is done for the two frequency spans, one of 50MHz and one of 100MHz, both centered on 4GHz. The Q-factor vs. WA data can then be used to calculate the Q-factor of the EUT by fitting a curve to the data set and rearranging for Q-factor. Both the 50MHz and 100MHz span give different curves, shown in Figure 4.

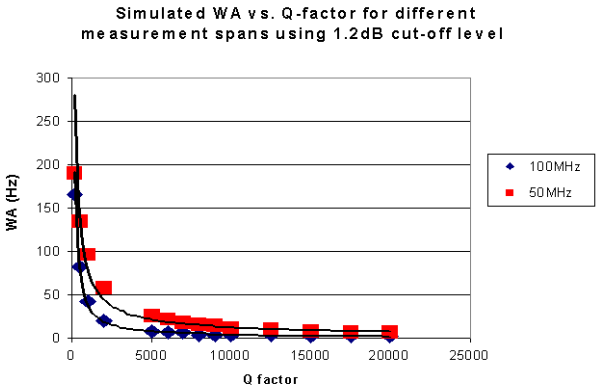

Figure 4: Q-factor plotted against simulated WA with a 50MHz measurement bandwidth showing different cut-off levels. The fitted lines are used to convert experimental WA values to Q-factors. The higher dB cut-off levels give wider WA.

It is worth noting that each cut-off level has its own WA vs. Q-factor relationship, and that the curve used fits the higher cut-off levels better.

IV. Experimental Results

Results are taken with five different aperture configurations to give five different values for SE to compare with the Q-factors obtained via the WA method. The aperture configurations (not including the "no holes" configuration) are shown in Figure 1. These give varying SE values. The SE values are then plotted against the Q-factors, which can be seen in Figure 5.

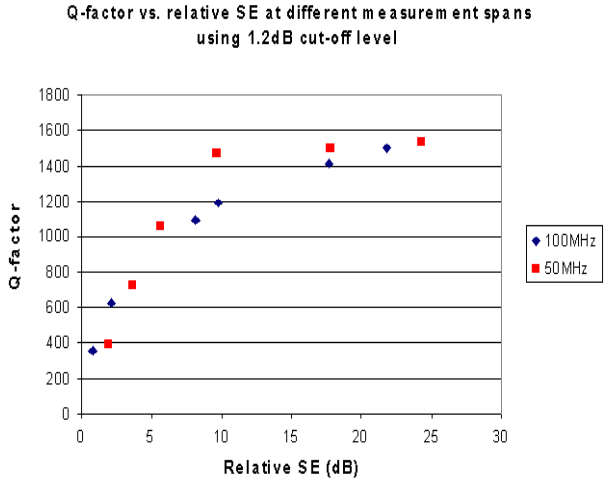

Figure 5: Q-factor vs. relative SE using the different aperture configurations. Red squares are the 50MHz measurement span while blue diamonds are the 100MHz measurement span.

It can be seen from Figure 5 that there is a monotonic relationship between Q-factor and SE. There are differences between both the different measurement bandwidths and the differing cut-off levels. It is worth noting that the abscissa on Figure 5 is relative SE rather than actual SE. The variations in the two figures are interesting as they indicate the variation between different scan bandwidths.

The shapes of the different scan bandwidth plots are also different. The 50MHz plot would not be so useful at higher relative SE values as it levels off above 25dB of relative shielding, reducing the Q-factor sensitivity for a given change in relative SE. The 100MHz plot shows no such leveling effect, and could be seen as being a more accurate way of obtaining Q-factors at higher levels of relative SE as the Q-factor sensitivity is larger.

From this it may be thought that the larger scan bandwidth is more beneficial as there are more resonant odes and therefore more information enclosed within the measurement span. However, the dependence of Q-factor on frequency makes having too wide a scan bandwidth detrimental to the results, as the Q-factor can change over the width of the scan.

Also measured was the Q-factor between two 19mm monopoles situated in the walls of the EUT. Power was transmitted into the EUT through one monopole and received from the other. Aperture configurations are changed on the front panel as previously and the EUT is still situated in the anechoic chamber. Figure 6 shows the

measured Q-factor vs. relative SE for the different methods used.

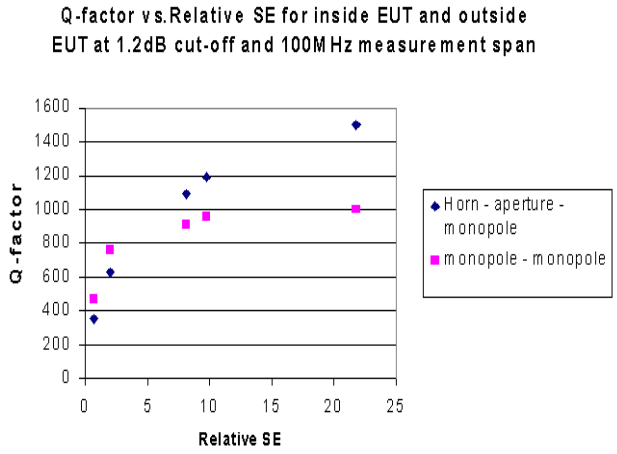

Figure 6: Q-factor against relative SE for different experiment layouts. The squares are from inside to inside the EUT while the diamonds are from outside to inside.

It can be seen from Figure 6 that the monopole to monopole plot is also monotonic. The Q-factor would be expected to be different as there are now two monopole antennas affecting the value of Q_4, the antenna Q-factor. The two measurement techniques are comparable at lower values of relative SE but deviation is seen at higher levels where the extra losses introduced by the second monopole antenna may be apparent.

V. CONCLUSIONS

It can be seen from Figure 5 that there is a relationship between measured Q-factor and relative Shielding Effectiveness. It has also become apparent that obtaining the Q-factor using the autocorrelation and WA method is dependent on the number of modes seen by the detecting instrument. using the WA method for obtaining Q-factor, a high cut-off value of 1.2dB is the most useful. A comparison can also be made between two different methods of obtaining the average Q-factor, seen in Figure 6, with the monopole to monopole method mirroring the external horn to monopole method for low values of relative SE. This work is currently being used to develop a measurement technique for obtaining aperture dominated SE measurements using the Q-factor measured between two antennas within the EUT. Such a technique would be of use in evaluating the SE of electrically large metallic equipment enclosures with modest levels of SE where the SE is dominated by the aperture losses.

REFERENCES

[1] C.L. Holloway, D. A. Hill, M. Sandroni, J.M. Ladbury, J. Coder, G. Koepke, A.C. Marvin, Y.He "*Use of Reverberation Chambers to Determine the Shielding Effectiveness of Physically Small, Electrically Large Enclosures and Cavities.*" IEEE Transactions on Electromagnetic Compatibility. (2008).

[2] A. C. Marvin, Y. He. "A study of enclosure shielding effectiveness measurement using frequency stirring in a mode-stirred chamber." *IEEE International Symposium on Electromagnetic Compatibility,* 2008

[3] D.A. Hill, M. T. Ma, A.R. Ondrejeka, B.F. Riddle, M.L. Crawford and R. T. Jhonk, "Aperture excitation of electrically large lossy cavities", *IEEE Trans. Electromag. Compat.*, Vol. 36, no. 3, pp. 169-178, Aug. 1994

[4] C. M. Butler, Y. Rhamat-Samii, R. Mittra. "Electromagnetic penetration through apertures in conducting surfaces" *IEEE Trans. on Antennas and Propagation,* Vol. AP-26, No.1 Jan 1978.

[5] C.L. Holloway, D. A. Hill, M. Sandroni, J.M. Ladbury, J. Coder, G. Koepke, A.C. Marvin, Y.He "Use of Reverberation Chambers to Determine the Shielding Effectiveness of Physically Small, Electrically Large Enclosures and Cavities." *IEEE Transactions on Electromagnetic Compatibility.* (2008).

[6] Yong Cui, "A new measure for evaluating shielding performance of an equipment enclosure at frequencies above 1GHz, *PhD Thesis, University of York,* 2007

[7] M. P. Robinson, J. Clegg, A. C. Marvin, "Radio frequency electromagnetic fields in large conducting enclosures: effects of apertures and human bodies on propagation and field-statistics", *IEEE Trans. Electromag. Compat.*, Vol 48, no. 2, pp. 304 – 310, May 2006